



Performance Evaluation of Eastman's Saflex® E Series Acoustic Interlayer

Pol D'Haene and Stijn Van de Vyver Eastman

Athanasios Poulos and Xavier Robin Free Field Technologies

Citation: D'Haene, P., Van de Vyver, S., Poulos, A., and Robin, X., "Performance Evaluation of Eastman's Saflex® E Series Acoustic Interlayer," SAE Technical Paper 2021-01-1054, 2021, doi:10.4271/2021-01-1054.

Abstract

In 2020, Eastman launched a new acoustic PVB interlayer for automotive laminated glass. This interlayer not only helps to protect driver and passengers from injuries during impact but also provides enhanced acoustic comfort in the car. This newly developed interlayer offers substantially improved acoustic performance in the high-frequency range that is typically associated with wind noise at higher vehicle speeds. To demonstrate the in-vehicle performance, finite element simulations have been carried out using wind noise as the principal source of excitation. The results confirm previously published data that the acoustic contribution overwhelms the turbulent part, having a larger contribution to the ultimate acoustical pressure level.

The acoustic insulation calculated is in excellent agreement with the static sound transmission loss data as measured

according to the ISO or ASTM norm. In cases where both the windscreens and front-side windows have a laminated structure, a large improvement in sound level is achieved by the acoustic interlayers, mainly in the 3,000 to 6,000 Hz frequency range. With the newly developed Saflex® E series interlayer, a further improvement in the higher frequency range is realized. In this simulation exercise, the relative contribution on the sound pressure level of laminated front-side windows in comparison with tempered glass has also been analyzed.

Besides, qualitatively similar results are obtained from an experimental simulation of rainfall at various intensities and angles of impact. With acoustic interlayers, a general reduction in sound level is measured, with an additional gain in the high-frequency range for the new E-series product. This behavior mirrors the performance level observed from the static sound transmission loss experiments.

Introduction

Cabin noise has been a topic of increasing interest for original equipment manufacturers (OEMs) in the last 20 years, mainly driven by the need for improved comfort and the growing importance of the intelligible voice commands. In general, motor noise, tire/road contact, and aerodynamically induced cabin noise are recognized as the primary sources contributing to the acoustic pressure level in a car. With the electrification of the power train (in hybrid and electric vehicles), the relative contribution of the latter two to the in-vehicle noise level, especially at the higher frequencies, will further increase.

Wind noise finds its origin in the turbulent flow existing around the external body of the car, especially when driving at high speeds. Flow disturbances created by the A-pillar, the wipers, and the side mirrors lead to fluctuations of the pressure field in the air layer surrounding the vehicle. These induce vibrations of the panels that constitute the envelope of the car as well as of the glazing surfaces, such as the windscreens and the side windows, resulting in the creation of acoustic air-pressure waves in the car's interior. Furthermore, these parts also form an important part of the transfer path for external

sound sources, being aero-acoustic in nature or originating from passing-by traffic.

For insulation from sounds of external origin (airborne noise) or for vibration damping (structural-borne noise), glazing surfaces for long have been a weak link. The need for transparency and the legal requirements of impact resistance of the windscreens more particularly, preclude the application of a sound absorption layer or a vibrational damping treatment as applied to the metallic parts of the vehicle. In recent years, more advanced polymeric polyvinyl butyral (PVB) interlayers have been developed to enable an increased absorption of sound energy of the glazing surfaces, resulting in a further reduction of the cabin noise level.

In this paper, an aero-acoustic numerical simulation study is presented to validate the effectiveness of the PVB interlayer to reduce the car's interior noise level and how this is linked to the viscoelastic properties of the material. In addition, the relative importance of both the windscreens and the side windows to the sound reduction is investigated. Finally, experimental results of a raindrop test are reported, revealing the importance of the interlayer composition on the reduction of the created sound.

General Background

A windscreens of a car consists of laminated glass made of a polymeric interlayer sandwiched between two glass panels (Figure 1), preventing objects from penetrating the vehicle on impact and securing the safety of driver and passengers. The film consists of a monolithic layer of PVB polymer with a thickness of approximately 760 μm .

In recent years, a multilayer PVB film has been developed which consists of three layers, for which the core layer has a different composition than the outer skin layers. This gives a better vibrational damping to the glass laminate, resulting in the attenuation of the amplitude of incident pressure waves (Figure 1).

Side windows, to date, primarily consist of tempered glass and only occasionally have a laminated structure.

The acoustic performance of laminated glass panels can be tested in different ways. For the lower frequencies, the damping efficiency is determined by means of a modal analysis or the measurement of frequency response functions (FRF) of a laminated glass panel. Figure 2 shows the outcome of such an experiment, for a configuration consisting out of two 2 mm glass panels with a size of 60 cm by 20 cm and laminated with an interlayer whose characteristics are specified in table 1. The results indicate a clear difference between the FRF of a monolithic PVB and an acoustic tri-layer construction revealing the highly damped behavior for the latter material. The performance at higher frequencies is estimated from a sound transmission loss experiment, carried out according to the ASTM

E90 [1] or EN ISO 10140-2 norm [2]. The efficiency of the acoustic interlayer is typically revealed by a shift of the coincidence frequency to a higher value and larger transmission loss numbers at this characteristic frequency.

Performance evaluation on a commercial vehicle is much more difficult to address. Typical testing procedures include track testing, static or dynamic testing in an anechoic chamber, or wind tunnel testing. This, irrespective of the test strategy, always requires the replacement of the windscreens and/or the side windows with the specific material to be investigated, leading to potential sources of error in the evaluation.

As an alternative to an experimental study, the approach described in this paper makes use of vibroacoustic simulations in which the mechanical material properties are introduced as frequency dependent viscoelastic moduli for the individual layers of the multilayer construction.

This process rules out the variability intrinsically associated with experimental testing. On the other hand, it eliminates the contribution of the transmission through the structural panels of the vehicle to the overall noise level in the cabin. Hence, results can only be compared relative to one another, mimicking the configuration of a wind tunnel test in which all panels (including the underbody) but the glazing surfaces are masked.

To validate this approach, the initial STL data, as acquired according to the ISO norm, are simulated. This practice not only allows for a verification of the methodology correlating the viscoelastic properties to the STL numbers but also enables an analysis of the sensitivity of the model setup and the mesh size on the precision of the calculations.

In a second step, the model is extended to the vibroacoustic simulation of a virtual vehicle cabin.

Materials

The PVB interlayers for which the sound attenuation properties are evaluated are listed in Table 1. All materials are commercially available products already implemented in standard vehicles.

The thickness of the core layer in the tri-layer products ranges between 15% and 20% of the total thickness, the latter being slightly larger than for the monolithic system to meet the impact performance requirement of the windscreens.

The viscoelastic properties of the individual layers are measured using a dynamic mechanical analyzer (TA Instruments DHR-3) equipped with a parallel plate geometry. Both storage and loss modulus are determined using a dynamic experiment for which the frequency is ranging from 0.01 to 80 Hz in a temperature interval increasing from -20°

FIGURE 1 Laminated glass construction

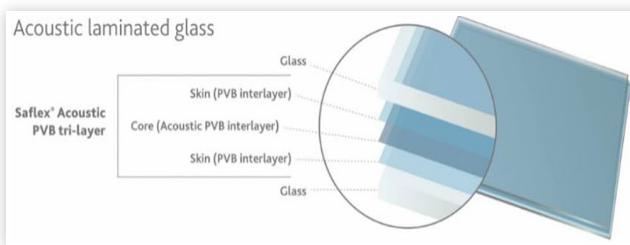


FIGURE 2 FRF functions for laminated glass panels

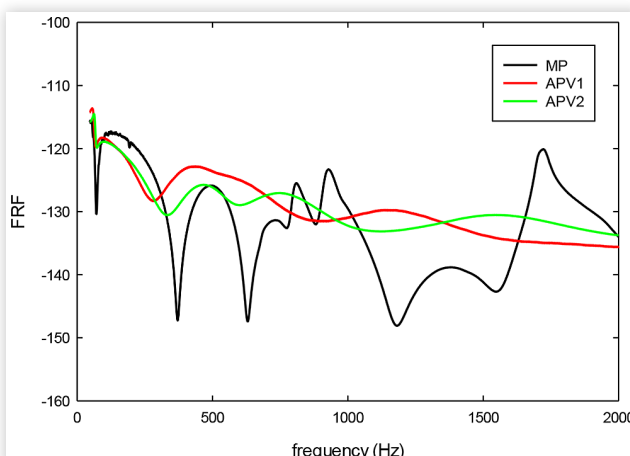
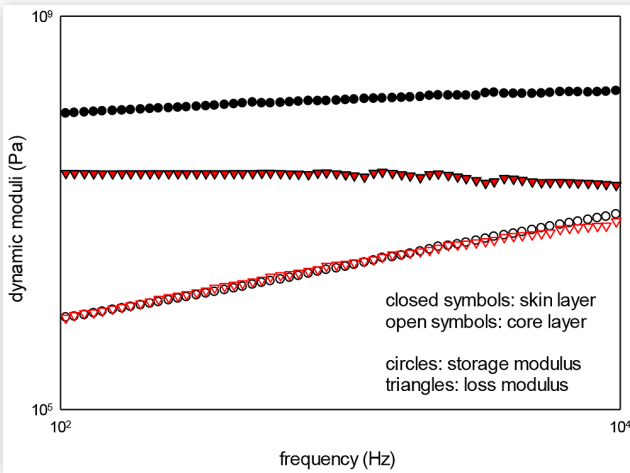


TABLE 1 List of materials tested

Material nomenclature	Construction	Thickness	Reference
Saflex® RB41	Monolithic	760 μm	MP
Saflex® Q series QF51	Tri-layer	840 μm	APV1
Saflex® E series EF51	Tri-layer	840 μm	APV2

FIGURE 3 Dynamic moduli for APV1 product

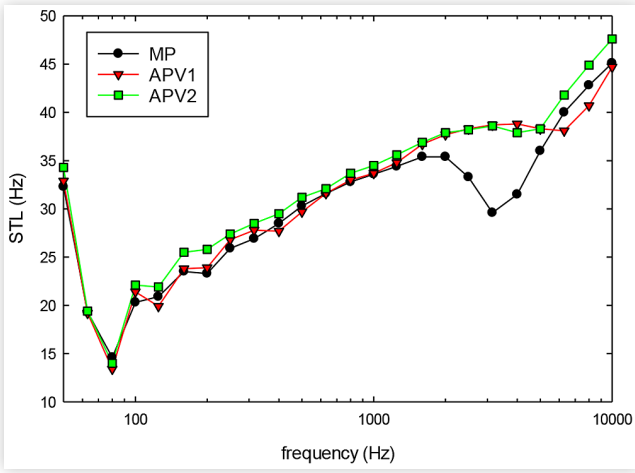
to 80°C. The applied strain is kept below the viscoelastic linearity limit, in accordance with the small deformation of the laminate upon bending under an applied acoustic pressure wave.

To expand the frequency interval to the range of acoustic interest, i.e., 100 to 10,000 Hz, the time-temperature superposition principle is applied. A typical curve of the dynamic moduli in this range, at a reference temperature of 20°C, is illustrated in Figure 3. The lower moduli numbers for the core layer are an expression of its softer behavior, responsible for the attenuation of the incident pressure waves. In comparison with the APV1 material, the APV2 product is characterized by a higher stiffness of the skin layer and an enhanced vibrational damping, as expressed by a larger $\tan(\delta)$ value at the glass transition temperature.

Acoustic Simulation of the STL Data

In an STL experiment, a laminated glass panel is positioned between two independent reverberant rooms or between a reverberant and an anechoic room. In the source room, a diffuse sound field is created at a constant power level. In both the receiver and the source rooms, the sound pressure level is recorded over a range of frequencies. The average difference in power measured between both chambers, taking into account the reverberation time of the receiving room is defined as the sound transmission loss. The characteristic curves of this property for the three PVB interlayers defined in Table 1 are plotted in Figure 4. The configuration is a combination of 2.1- and 1.6-mm thick glass panels.

The effect of the softer core layer is obvious. Due to an overall decrease in stiffness of the laminate in the case of the acoustic interlayers, the coincidence frequency is shifted to a higher value. The damping of the interlayer, related to the value of the glass transition temperature of the core, is reflected in the higher values of the STL at the coincidence point. However, a lower value of the coincidence frequency is beneficial for the performance at higher frequencies, taking advantage of the steep increase of the STL curve at frequencies

FIGURE 4 STL data for interlayers defined in table 1

exceeding this critical point. This explains the reduced performance of the APV1 product versus the monolithic material at frequencies above 5000 Hz. This drawback has been resolved for the APV2 formulation. It has a coincidence frequency closer to the corresponding value of MP while maintaining the damping of APV1, resulting in an enhanced performance in the frequency range beyond the coincidence region. This can be explained by the better bending resistance of the APV2 based laminate, induced by the increased stiffness of the skin layers.

This STL experiment is modelled using Actran® [15]. The set-up for the simulation is shown in figure 5.

A multilayered panel is embedded into a baffled structure. A diffuse sound field is applied on one side of the panel. The other side, being an acoustic volume, is meshed using 3D finite elements. The far field is meshed using either infinite elements or with a APML (adaptive perfectly matched layer), depending on the frequency range of interest. At higher frequencies an APML is preferred because of the lower running cost. The laminate is modelled using solid shells, adopting one element over the thickness of each individual layer. Depending on the frequency range of interest the mesh size is adapted always ensuring the presence of five quadratic elements per wavelength, as presented in Figure 6. The picture also illustrates

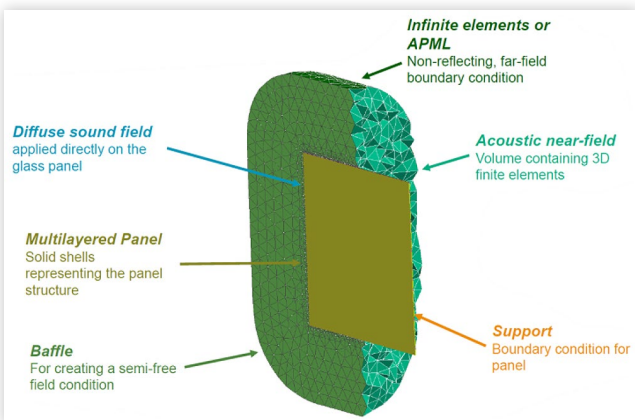
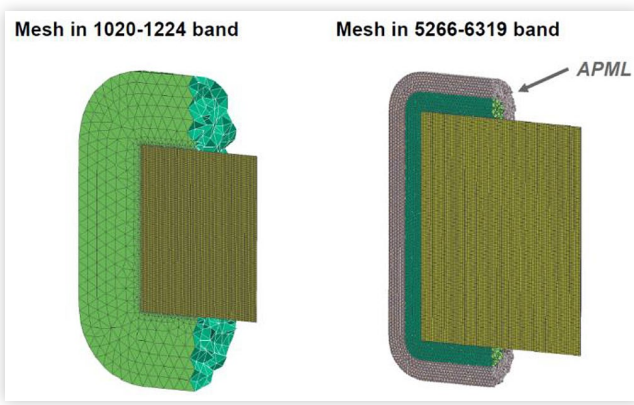
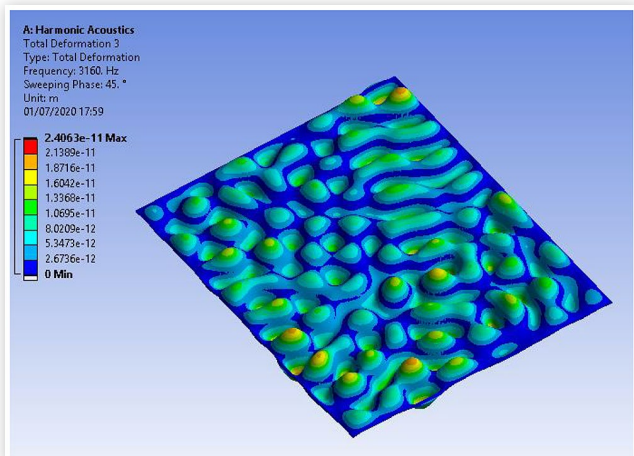
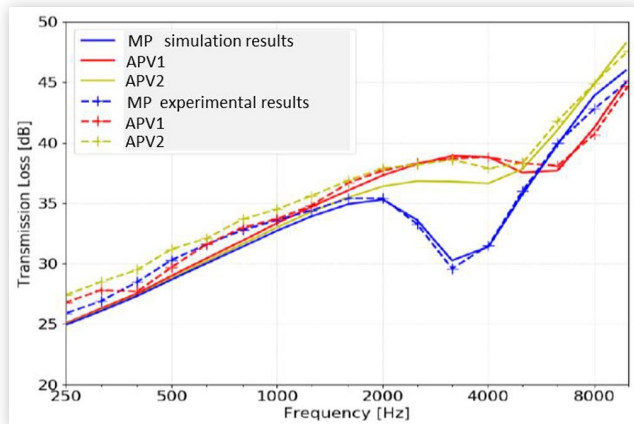
FIGURE 5 Set up of FE simulation for STL experiments

FIGURE 6 Mesh size for mid and high frequency range

the change in set-up using infinite elements at low frequencies and the APML layer in the higher frequency range.

As the FE approach is used for frequencies up to 10000 Hz, the memory requirements and the run times increased exponentially with increasing frequency. Hence, at higher frequencies, advantage can be taken of the symmetry of the configuration to simplify the model, adopting a half or quarter model approach. A comparison of the predictions of the different models only points to differences in the lower frequency range. For simulations exceeding 1,000 Hz the values of the full, half or quarter models coincide. The deviation at lower frequencies is not surprising considering the relatively small size of the panel compared to the wavelength of the acoustic signal and the presence of anti-symmetric excitations. As an illustration, Figure 7 compares the size of the calculated wave at a frequency of 3,160 Hz to the dimensions of the panel indicating the presence of multiple wavelengths over both the width and the length of the laminate. In addition, the modal density at low frequencies is rather small by which individual modes have a larger impact on the calculated result, an effect which decreases with increasing modal densities leading to smaller differences when applying symmetry conditions. Both phenomena also explain the

FIGURE 7 Calculated deformation of glass panel due to an imposed sound pressure wave (glass: 8 mm, freq.=3160 Hz)**FIGURE 8** Comparison between experimental STL data and predicted values using ACTRAN

negligible influence the boundary conditions have on the laminate bending in the higher frequency range.

Figure 8 shows a comparison between the results of the STL experiments and the predicted values obtained from the ACTRAN simulation.

In general, a good agreement is obtained between the measured and the calculated values up to the highest frequencies. The prediction of the coincidence frequency is also accurate, ensuring the exact order in performance of the different interlayers in the higher frequency regime. For all materials the model slightly underestimates the STL numbers in the zone where the mass law governs the acoustic performance. Depending on the glass thickness and the interlayer type this range extends from approx. 200 Hz to 2,000 Hz (monolithic) or 3,000 Hz (acoustic interlayers). This deficiency is also observed using 3D models developed in other FE simulation packages such as Ansys®. Although the weight of the construction governs the sound attenuation in that frequency interval some effect of increased damping tends to improve the transmission loss, a phenomenon not revealed in the numerical simulations. In the coincidence region (2,000 to 4,000 Hz) and, for APV2 in particular, the simulation under-predicts the performance. The origin of this deviation is currently not well understood, but it is important because it is an interval of great influence for voice recognition devices.

From these simulations it can be concluded that the ACTRAN model enables the prediction of the experimental transmission loss data starting from the dynamic mechanical properties of the interlayer. Based on these conclusions, the set-up is further expanded towards a vibroacoustic model to determine the relative influence of the type of interlayer on the interior noise level in a vehicle's cabin.

Influence of the Interlayer Structure on In-Vehicle Noise Levels

The value of virtual modelling has been proven extensively in literature over the last 10 years. In view of the content of this

paper, literature on aeroacoustic and vibroacoustic simulations can be summarized under three different topics.

The first research field of interest focuses on CFD simulations required to determine the acoustic pressure fluctuations induced by wind noise. Unsteady-state modeling (either based on lattice Boltzmann or on finite volumes methodology) using a compressible fluid solver leads to the most accurate results but requires large quantities of computer resources and time. Hence, this approach is predominantly limited to final performance assessments on an already optimized design. An alternative pathway, allowing a faster calculation, is based on a steady state RANS simulation from which turbulent velocity fluctuations (using the SNGR - Stochastic Noise Generation and Radiation - approach) can be constructed that can be used to compute aeroacoustic sources applying Lighthill's analogy. While this method is currently not yet able to reproduce absolute noise levels, the numerical approach can be applied to quickly assess different virtual design alternatives related to aero-dynamically induced interior noise values [3,4,5].

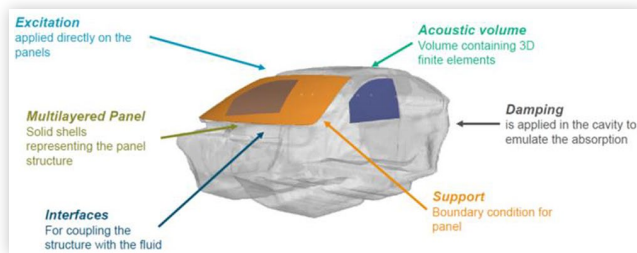
The second subject of interest is the methodology to distinguish between the effect of the turbulent and acoustic contribution to the noise level in a car. The total pressure fluctuations due to wind noise, acting either on a panel or a glass window, include both convective and acoustic pressure fluctuations. These pressure variations are different from a wavelength perspective (wavelength of the acoustic fluctuation is longer than the convective wavelength) and from an amplitude point of view with the energy level for the convective component being larger. Techniques are described in literature to distinguish between both contributions, both experimentally as well as numerically [6,7,8,9,10].

Finally, in a last selection of papers, being an intrinsic part of the previously referenced cases and serving as a validation for the numerical model, focus of the research work is on the assessment of the effect the turbulence inducing parts (such as the A-pillar, side mirrors, wipers, etc.) can have on the internal noise level. In that respect and as an example, Van Herpe et al. have carried out a combined aero/vibro-acoustic simulation to study the contribution of side laminated windows and the windscreens to the noise level in a vehicle. The turbulent flow field is computed using an unsteady simulation based on the Lattice Boltzmann approach, and the vibroacoustic transmission is calculated using Actran®. Their main conclusion is that the contribution to the in-vehicle noise level is predominantly influenced by the transmission through the side laminated windows except in the lower frequency range where the transmission through the windscreens becomes more significant. Note however, that the contribution of the non-glass elements is considered to be at least as important as the glazing component. The upper frequency limit of their simulations is limited to 1,600 Hz. This range is extended to frequencies beyond the coincidence limit in this paper [11].

As stated in the introduction, the aim of this investigation is to evaluate the effect the PVB interlayer has on the sound pressure level in the car with the wind noise as sole contributor, excluding any other potential source. To this purpose, a vibroacoustic simulation approach is applied.

The study utilizes a virtual car model, kindly provided by FFT, constituting the acoustic volume. It is coupled to both

FIGURE 9 Setup for vibroacoustic simulation



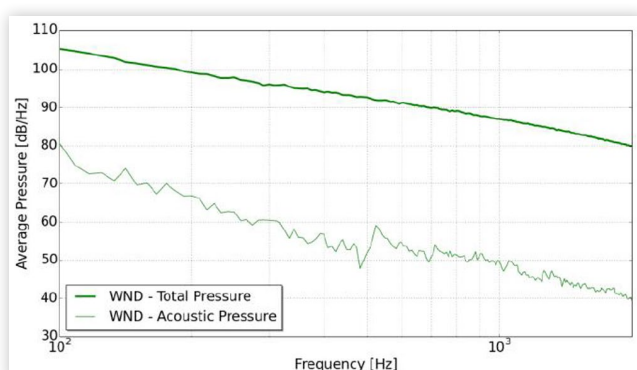
windscreens and front-side laminated windows by means of a two-way interaction (Figure 9).

Similar to the STL simulations, the laminated glass surfaces are represented as multilayered parts using solid shells representing the panel structure. The panels are simply supported at the boundaries, which only have a real influence at the lower frequencies and are of less interest in this study. The other structural panels of the body are defined to be rigid. Vibro-acoustic simulations are carried out to calculate the sound pressure level in the cavity. The response is measured locally by positioning virtual microphones at different locations in the car. The sound pressure level at these microphones is averaged to get a better idea of the global response and this value is reported in this paper. Absorption effects due to the internal trims are modelled by applying a damping in the form of a complex sound speed. The damping factor used is computed by utilizing reverberation time values (RT60), typical of a luxury sedan [16]. Despite the size of the mesh, (which in the case of high-frequency simulations grows to large values), all FE simulations are carried out on the full model.

Both the front-side glazing and the windshield are excited with an equivalent aerodynamic spectrum, distinguishing between the turbulent and the aero-acoustic contribution (figure 10) [6]. The turbulent contribution is not shown on the figure but is very close to the total pressure, overwhelming the acoustical fraction. Also note that for this study, the spectrum is extended to 10000 Hz.

The turbulent part of the excitation is based on the turbulent boundary-layer theory. As in this study there is no real interest in the effect the vehicles' contour could have on the

FIGURE 10 Excitation spectrum for windscreens and side laminated windows



turbulent flow field and hence on the interior noise, the excitation level is gathered from another aeroacoustic study adopting an unsteady CFD simulation. Due to confidentiality reasons the spatial distribution is not derived from this model. Instead it is based on the asymptotic approach of the Corcos model including the Elswick correction, which is especially valid in the high-frequency range and at lower speed levels [13].

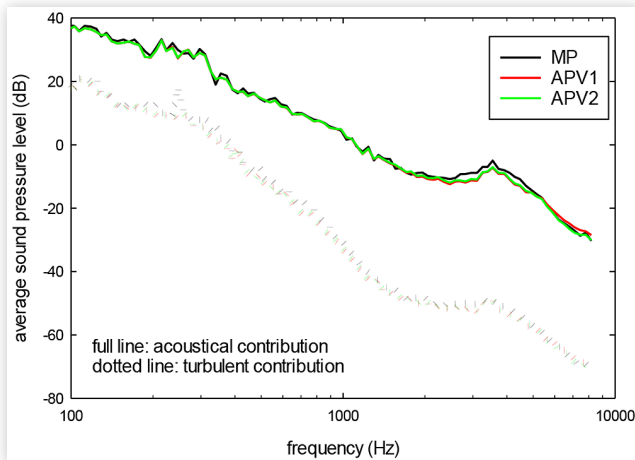
The acoustic part of the excitation makes use of a diffuse sound field, for which again the power spectrum is obtained from the unsteady CFD simulation (figure 10). No spatial correlation function is further associated with this contribution. Due to limitations in the mesh size and the time steps adapted in CFD modeling, energy levels at higher frequencies tend to be underpredicted. Therefore, in that range, the amplitude of the spectrum is corrected to more realistic values. Remark that the amplitude of the turbulent wave is much higher than for the acoustic wave, which corresponds to the findings described elsewhere [8,9,10].

Two separate cases, differing in the type of glazing having a laminated configuration, are investigated.

For the first set of simulations both the windscreens and the front-side windows have a laminated structure, each comprising an identical interlayer. The results of these calculations, represented as the mean square acoustic pressure averaged over the entire cavity, are shown in figure 11.

The total pressure is built from two contributions for which the acoustic part overwhelms the turbulent fraction. Note that, for clarity reasons, the total pressure is not plotted on the graph as it coincides completely with the acoustic curve. Despite their lower energy content, the acoustic waves show a larger transmission efficiency, related to the greater similarity of the acoustic wavelength with the bending waves induced in the laminated glass panel. Due to the higher importance of the acoustic contribution interacting with the panel in the form of a diffuse sound field, it is not surprising that the combined excitation results in an internal acoustic response in close agreement with the shape of the STL response. The APV2 product approximates the monolithic material at high frequencies, and results in an overall lower noise level as compared to the APV1 interlayer. In the

FIGURE 12 Average pressure level in the cabin (windscreen only laminated)



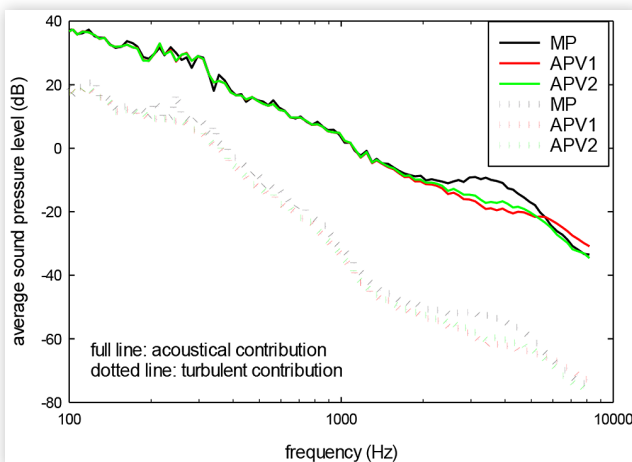
mid-frequency range (2,000 to 5,000 Hz) both acoustic products are equivalent, considering the model's deficiency to accurately predict the STL values in that range as is illustrated in Figure 8.

In a second phase, the front-side laminated windows are replaced by a tempered glass panel with a thickness of 4 mm (figure 12).

It is obvious that the effectiveness of the acoustic interlayers to reduce the interior noise level is strongly decreased, as the performance can hardly be distinguished from the monolithic layer. Slightly lower pressure levels can still be noticed in the 2,000 to 4,000 Hz range; however, at higher frequencies, hardly any difference is noticeable.

These data clearly suggest, considering the simplifications made in the simulations, that laminated side windows are more efficient in reducing noise level in the cabin originating from aeroacoustic sound sources. This confirms the data presented by Van Herp et al., showing similar conclusions over a more limited frequency range [11].

FIGURE 11 Average pressure level in the cabin (windscreen and side windows laminated)



Raindrop Testing

In the previous sections, it was illustrated that acoustic interlayers effectively dampen sound propagation in laminated automotive glass reducing the wind noise level within the cabin considerably and resulting in an increased passenger comfort. Due to the growing interest in automotive sunroofs, rain noise can, in certain climatological conditions, also be considered as an additional contributor to internal noise. The effect the interlayer can have on this structural-borne noise source is evaluated by means of a series of artificial rain drop experiments according to ISO 10140-1 (2016). The materials that are evaluated are identical to those mentioned in table 1.

Laminated glass panels are mounted, horizontally and slightly inclined, in the opening between two rooms, positioned vertically above one another. In the upper room, artificial rain is generated by dropping water onto the laminate

FIGURE 13 Sound pressure levels under heavy raindrop simulations

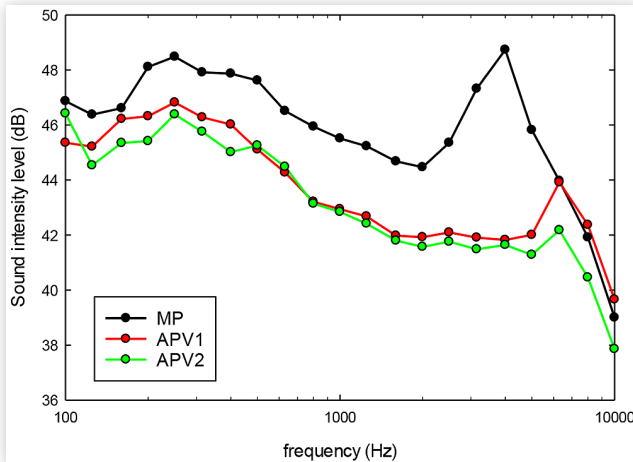
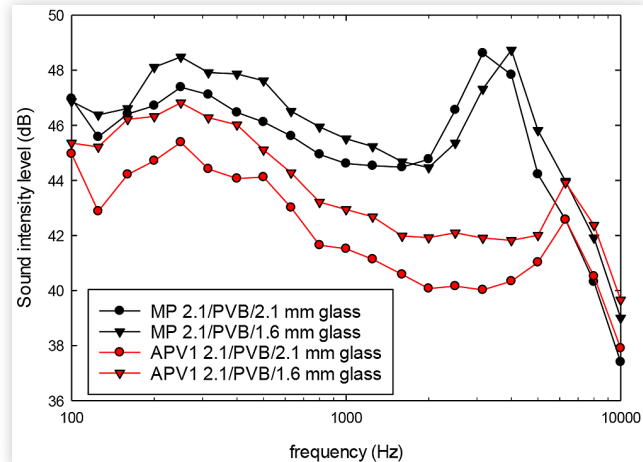


FIGURE 14 Effect of glass thickness on raindrop induced noise levels



through a perforated plate. In the receiving chamber, a reverbation room, the sound pressure levels are recorded as a function of frequency. Depending on the hole size in the perforated plate heavy rain or cloud burst circumstances can be simulated.

In figure 13 the recorded sound intensity levels are presented for a heavy rain drop experiment on a glass laminate consisting of 2.1 mm and 1.6 mm glass panels. At first glance, the behavior mimics the performance level already noticed in the STL experiments. For the acoustic interlayers, a lower sound pressure level is measured, the coincidence frequency is shifted to higher values and in the coincidence region a higher damping occurs. It is striking that in the frequency interval in which the mass law governs the acoustical performance, a reduced sound intensity level is measured in case of the acoustic products. This effect was already apparent in the STL results but is more expressed for the raindrop simulation tests.

When analyzing the data from figure 11 and figure 12 in more detail, a similar difference of 2 dB is noticed for the turbulent component of the spectrum up to the coincidence frequency. This supports the conclusion that damping also has an effect in the mass law governed region and becomes more significant in case of structural-borne noise compared to airborne noise transmission.

The effect of glass thickness for a monolithic and an acoustic interlayer is illustrated in figure 14. Total glass thicknesses of the constructions are respectively 3.7 and 4.2 mm. The results confirm the expectations that a higher mass results in lower sound pressure level. However, the data also indicate that an acoustic interlayer enables a decrease in the glass thickness of more than 10%, without having a negative impact on the interior noise level created by heavy rainfall. These observations are not only valid for a sunroof but can be extended to the windscreens, for which even higher sound pressure levels are expected due to the higher impact velocity of the raindrops on the glass surface. Power input of rainfall is expected to increase strongly with increasing intensity, both for artificial as well as for natural rain. This increase can be related to a

higher raindrop diameter and to a higher dropdown velocity, hence an enhanced impact speed [14].

Conclusions

Vibroacoustic simulations are explored as a means to evaluate the effect of the PVB interlayer, characterized by its viscoelastic properties, on the wind noise-induced sound pressure level in a car. The methodology is successfully applied for predicting the more static sound transmission loss experimental data. Both experimental and simulation data indicate that an acoustical interlayer with a higher skin stiffness helps to correct the deficiency of existing acoustic interlayers in the higher frequency range to a level exceeding the STL values of the monolithic product without any loss in performance in the coincidence region.

This behavior is confirmed for in-vehicle applications for which an identical performance is calculated. This similarity can be attributed to the overwhelming effect of the aero-acoustic component over the turbulent part towards the interior noise level. In addition, this study also demonstrates that laminated side windows have a higher efficiency than the windscreens, for shielding a cabin from aeroacoustically induced noise sources.

In addition, similar conclusions are derived from experimental raindrop simulations. The advantage of acoustic interlayers is clearly demonstrated, including a surprisingly large effect in the mass law governed frequency range. This allows a reduction of glass thickness of more than 10% without any significant deterioration of the sound quality in the car cabin.

Future simulations will further explore the value of these observations, by evaluating more exactly the effect of the excitation spectra for side laminated windows, windscreens, and sunroofs individually, including their spatial distribution. Such evaluations will better determine the individual contribution of the glass components to the internal acoustic pressure level in a commercial vehicle.

Acknowledgements

This work has been carried out in collaboration with Free Field Technologies (FFT) and with Daidalos Peutz, for which we are very grateful. Special thanks go to Thanos Poulos (FFT) and Paul Mees and Theo Sheers (Daidalos Peutz) for the fruitful discussions.

References

1. ASTM E 90, "Laboratory Measurement of Airborne Sound Transmission Loss of Building Partitions and Elements."
2. EN ISO 10140-2, Acoustics-Laboratory Measurement of Sound Insulation of Building Elements - Part 2: Measurement of Airborne Sound Insulation (ISO 10140-2:2010).
3. Mazeaud, B., Chronéer, Z., Karlsson, M., Yao, H.-D. et al., "Application of SNGR method to compute Aero-Vibro-Acoustics of Heavy-Duty Rear-View Mirrors," in *Presented at 25th AIAA/CEAS Aeroacoustics Conference*, Delft, May 2019.
4. Liu, Y., Lu, W., Zhang, Q., Wang, X. et al., "An Efficient Method for Prediction of the Flow-Induced Vehicle Interior Noise," *J. of Physics: Conference Series* 1650 (2020).
5. de Brye, B., Poulos, A., Legendre, C., and Lielens, G., "A Cost-Effective Computational Technique for Aeroacoustic Noise Prediction Using the SNGR Method," in *Presented at ISMA 2020*, Leuven, Belgium, 2020.
6. Ganty, B., Copiello, D., Detandt, Y., and Jeong, C., "A Method to Identify the Acoustic Contribution in Pressure Fluctuations Acting on a Realistic Car's Side Window," in *Presented at Internoise 2015*, San Francisco, 2015.
7. Jacqmot, J., Detandt, Y., Lielens, G., and Copiello, D., "Vibro-Aero-Acoustic Simulation of Side Mirror Wind Noise and Strategies to Evaluate Pressure Contributions," *ISMA 2016*.
8. He, Y., Schröder, S., Shi, Z., Blumrich, R. et al., "Windnoise Source Filtering and Transmission Study Through a Side Glass of DrivAer Model," *Applied Acoustics* 160 (2020).
9. He, Y., Liu, Y., Wen, S., and Yang, Z., "Separation of Convective and Acoustic Pressure Fluctuations on the Front Side Window of DrivAer Model Based on Pellicular Mode Decomposition," *Applied Acoustics* 174 (2021).
10. Yuan, H., Yang, Z., Wang, Y., Fan, Y. et al., "Experimental Analysis of Hydrodynamic and Acoustic Pressure on Automotive Front Side Window," *Journal of Sound and Vibration* (2020): 476.
11. Van Herpe, F., D'Udekem, D., Jacqmot, J., and Kouzaiha, R., "Vibro-Acoustic Simulation of Side Windows and Windshield Excited by Realistic CFD Turbulent Flows Including Car Cavity," SAE Technical Paper 2012-01-1521 (2012). <https://doi.org/10.4271/2012-01-1521>.
12. EN ISO 10140-1, Acoustics-Laboratory Measurement of Sound Insulation of Building Elements - Part 1: Application Rules for Specific Products (ISO 10140-1:2016).
13. Corcos, G.M., "Resolution of Pressure in Turbulence," *The Journal of the Acoustical Society of America* 35 (1963): 2.
14. Hopkins, C., "Sound Insulation," Elsevier, Chapter 3: Measurement, 2007.
15. Free Field Technologies S.A. Actran 2021 User's Manual, 2020.
16. Bennetts, A. and Morris-Kirby, R., "RT60: Its Use as an Optimizer in Automotive Cabins", Whitepaper, Bay Systems Ltd., 2004.

Contact Information

Pol D'Haene
+32 9243 6383
ppdhae@eastman.com